DOI: 10.2478/rjti-2025-0003

ROMANIAN JOURNAL
OF TRANSPORT INFRASTRUCTURE

COMPOSITE STEEL-CONCRETE ORTHOTROPIC DECKS

Chindriș I. Ionuț*, Ph.D Student Eng. Assistant Professor, Department of Railways, Roads and Bridges, Faculty of Civil Engineering, Technical University of Cluj-Napoca, e-mail: ionut.chindris@cfdp.utcluj.ro (author for correspondence)
Hoda Tudor, Ph.D Student Eng., Department of Railways, Roads and Bridges, Faculty of Civil Engineering, Technical University of Cluj-Napoca, e-mail: Tudor.Hoda@infra.utcluj.ro
Iliescu Mihai, Ph.D Professor, Department of Railways, Roads and Bridges, Faculty of Civil Engineering, Technical University of Cluj-Napoca, e-mail: Mihai.Iliescu@infra.utcluj.ro
Moga Cătălin, Ph.D Eng. Lecturer, Department of Structures, Faculty of Civil Engineering, Technical University of Cluj-Napoca, e-mail: catalin.moga@dst.utcluj.ro

Abstract

This paper proposes a calculation methodology for composite steel-concrete orthotropic deck, adapted from the European design standards EN 1993-1-5, EN 1994-1-1, and EN 1994-2. The construction solutions analyzed include steel girders with a monolithic reinforced concrete slab cast over orthotropic plating, providing advantages such as increased bending and torsional stiffness, elimination of the need for bracing, and improved corrosion protection. The shear lag effect is evaluated at both serviceability (SLS) and ultimate limit states (ULS) using the models recommended by EN 1993-1-5. A case study illustrates the application of the method on a 38 m-span footbridge, where the effective plate width and the interaction between shear lag and local buckling are analyzed. Stresses due to concrete shrinkage, creep, and thermal effects are also considered. The results demonstrate that the entire plate width remains active, with negligible differences between effective and gross areas. The conclusions highlight the efficiency of the composite orthotropic solution in bridge design.

Keywords: orthotropic deck, composite structures, shear lag, bridges, footway bridge

1. INTRODUCTION

Composite steel-concrete structures provide efficient solutions for most types of construction, including civil and industrial buildings, and bridges.

Currently, the following construction solutions are used:

- Steel beams with a monolithic reinforced concrete slab poured on removable formwork;
- Steel beams with a monolithic reinforced concrete slab cast over pre-slabs, which also serve as formwork during concrete pouring;
- Steel beams with a monolithic reinforced concrete slab poured on folded plates, which serve both as permanent formwork and structural elements;

- Steel beams with prefabricated slabs, monolithic in areas equipped with cooperation elements (typically elastic connectors);
- Steel beams with orthotropic plate-type metal deck and a monolithic reinforced concrete slab.

The use of orthotropic composite deck plates in road bridges and pedestrian walkways structures can be an advantageous solution for the following reasons:

- Increases bending and torsional stiffness of the composite beam;
- The metal plating, designed as an orthotropic plate, serves as formwork for pouring the monolithic reinforced concrete slab;
- Elimination of upper flange bracing, ensuring lateral-torsional stability during construction;
- For relatively lightweight superstructures, the deck can be installed as a single piece without temporary scaffolding in the riverbed.

This study presents a methodology for analyzing composite steel-concrete orthotropic decks. The approach is based on the Eurocode provisions for plated steel elements (SR EN 1993-1-5:2008) and composite structures (SR EN 1994-1-1:2006 and SR EN 1994-2:2006), as no dedicated standard currently addresses this specific type of structure.

The focus of the paper lies in the theoretical and numerical investigation of composite orthotropic decks. The main objective is to extend the applicability of the Eurocodes to complex orthotropic geometries and to propose a practical design methodology suitable for engineering applications.

2. PREMISES AND METHODOLOGY

This study presents a theoretical and numerical approach to the analysis of composite steel-concrete orthotropic decks, The methodology proposed here is based on current European standards — EN 1993-1-5 for plated steel elements and EN 1994-1-1 and EN 1994-2 for composite steel-concrete structures.

2.1 Premises and Assumptions

The following key premises are considered throughout this work:

- The structure consists of a composite section made up of an orthotropic steel plate and a monolithic reinforced concrete slab;
- Linear-elastic behavior is assumed for serviceability limit state (SLS), and elastic-plastic considerations are included at ultimate limit state (ULS);

- The analysis is based on Eurocode prescriptions, with adjustments made to accommodate the specific behavior of orthotropic configurations;

2.2 Methodological Approach

The methodology combines code-based design procedures with analytical calculations specific to the geometry and constraints of orthotropic decks. The steps include:

- Effective Width Evaluation at SLS
- Shear Lag and Buckling Interaction at ULS
- Equivalent Plate Modeling
- Stress Analysis due to Concrete Creep, Shrinkage, and Thermal Effects:

2.3 Theoretical Objectives

The analytical procedures aim to verify whether:

- The full width of the orthotropic deck plate remains active under both SLS and ULS conditions;
- Simplified modeling assumptions (equivalent flat plates) provide accurate results for stress and stiffness predictions;
- The effects of shear lag and plate buckling are sufficiently limited for practical design purposes;
- Additional time-dependent and thermal stresses are significant enough to require consideration in design.

3. DESIGN BASIS OF COMPOSITE STRUCTURES

3.1. Modular ratio

To determine the sectional characteristics of composite sections, the transformed section method is used. This method converts the non-homogeneous steel-concrete cross-section into an equivalent homogeneous section by transforming the concrete slab section into an equivalent steel section.

This transformation is achieved using the modular ratio, defined as the ratio of the modulus of elasticity of steel to that of concrete, which varies based on the type of loading (short-term or long-term) [1, 2].

For short-term loading:

$$n_0 = \frac{E_a}{E_{cm}} \tag{1}$$

where: E_a - is the modulus of elasticity of steel;

E_{cm} - is the modulus of elasticity of the concrete used in slab.

For permanent and long-term loading, the modular ratio accounts for concrete creep and is calculated as:

$$n_L = n_0 \cdot (1 + \psi_L \cdot \varphi(t, t_0)) \tag{2}$$

where: ψ_L - is the multiplier for concrete creep (1.1 for permanent loading, 0.55 for shrinkage effects);

$\varphi(t, t_0)$ - is the creep coefficient [1, 2]

3.2. Equivalent Steel Area of the Concrete Section

The equivalent area of the concrete section converted into steel is:

$$A_{eq} = \frac{A_c}{n} \tag{3}$$

where: A_c - is the area of the concrete section;

n - is the equivalence coefficient corresponding to the load under consideration.

4. COMPOSITE GIRDERS WITH ORTHOTROPIC DECK

For pedestrian walkways and bridges, open or partially closed box girders with a monolithic reinforced concrete slab can be adopted (Figure 1).

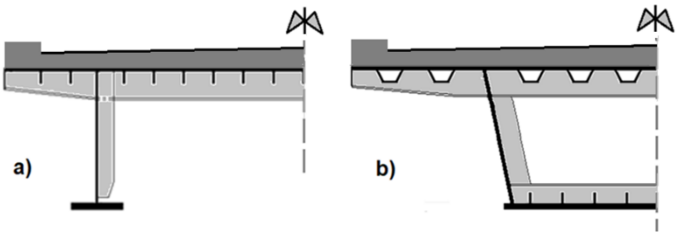

Figure 1. Girders with orthotropic deck and reinforced concrete slab:
a) Open section; b) Box girder

This solution offers the following advantages:

- Increases bending and torsional stiffness of the girder;
- The orthotropic metal plating serves as formwork for the monolithic reinforced concrete slab;
- The concrete slab enhances deck rigidity;

- No need for upper flange bracing to ensure lateral buckling stability during assembly; [3, 4]
- Improves dynamic behavior parameters for pedestrian walkways, enhancing comfort for pedestrian traffic;
- Protects the upper flanges against corrosion.

4.1. Elastic Shear Lag Effect at Serviceability Limit State and Fatigue (SLS)

In [5], shear lag is accounted for using the effective[s] width of the flange:

$$b_{eff} = \beta \cdot b_0 \tag{4}$$

where β is an efficiency factor given in Table 1 [5]

Table 1. Evaluation of Coefficient β

Location for verification	β - value	k
Regions of positive (sagging) bending	$\beta = \beta_1 = \dfrac{1}{1+6.4 \cdot k^2}$	0.02 - 0.70
	$\beta = \beta_1 = \dfrac{1}{5.9 \cdot k}$	> 0.70
Regions of negative (hogging) bending	$\beta = \beta_2 = \dfrac{1}{1+6.0 \cdot \left(k - \dfrac{1}{2500 \cdot k}\right) + 1.6 \cdot k^2}$	0.02 - 0.70
	$\beta = \beta_2 = \dfrac{1}{8.6 \cdot k}$	> 0.70
Linear bending on end supports	$\beta_0 = \left(0.55 + \dfrac{0.025}{k}\right) \cdot \beta_1;$ but $\beta_0 < \beta_1$	all *k* values
Cantilever	$\beta = \beta_2$ at support and at the end	all *k* values
where: $k = \dfrac{\alpha_0 \cdot b_0}{L_e}$; $\alpha_0 = \sqrt{1 + \dfrac{\sum A_{s\ell}}{b_0 \cdot t_f}}$		

The effective length L_e is defined in Figure 2.

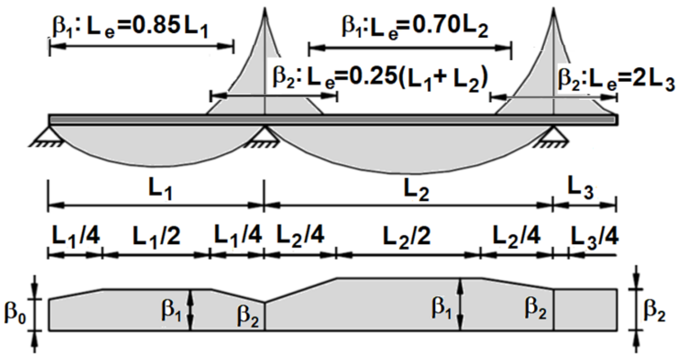

Figure 2. Definition of the effective length L_e (Figure 3.1 from [5])

According to [5], shear lag in flanges may be neglected if $b_0 < L_e/50$.

4.2. Shear Lag Effect for Ultimate Limit States (ULS)

For flanges in compression at ULS, the plate buckling effects may occur alongside shear lag effects. [5]

At ULS, shear lag effects can be determined as follows:

a) Elastic shear lag effects as for SLS and fatigue;

b) Combined effects of shear lag and plate buckling;

c) Elastic-plastic shear lag effects allowing for limited plastic strains.

EN 1993-1-5 proposes two models for interaction between shear lag and plate buckling:

Model 1 (Method b):

- Calculate the effective^p area for plate buckling;
- Define an effective^p stiffening ratio α_0^* to replace the stiffened ratio α_0 and calculate the reduction factor β_{ult} (using Table 1) instead of β, where:

$$\alpha_0^* = \sqrt{\frac{A_{c.eff}}{b_0 t}} \tag{5}$$

- Calculate the effective area A_{eff} considering shear lag and plate buckling:

$$A_{eff} = \beta_{ult} \cdot A_{c.eff} \tag{6}$$

Model 2 (Method c) - recommended in [5]:

- Apply an elastoplastic reduction factor $\beta^k \geq \beta$ directly to the effective^p area of the compression flange, where k is based on α_0:

$$A_{eff} = \beta^k \cdot A_{c.eff} \geq A_{c.eff} \cdot \beta \tag{7.a}$$

or:

$$A_{eff} = \beta_{e-p} \cdot A_{c.eff} \tag{7.b}$$

where $\beta_{e-p} = \max(\beta^k; \beta)$.

It is recommended to apply the reduction factor to the plate thickness, not the width.

Numerical examples of shear lag effects are presented in [6, 7, 8].

4.3. Evaluation of Stresses in Concrete Slab and Steel Plate

The reinforced concrete slab, structurally connected to the orthotropic steel plate through shear connectors (Figure 3), can be replaced by an equivalent continuous steel plate with thickness calculated as:

$$t_{eq.}^{c} = \frac{A_{c.eff}}{n \cdot (B/2)} = \frac{t_c \cdot \sum b_{eff}}{n \cdot (0.5B)} \tag{8}$$

where: $n = \begin{cases} n_0 = \dfrac{E_a}{E_{cm}} & \text{– for short – term actions} \\ n_L = n_0 \cdot (1 + \psi_L \cdot \phi(t, t_0)) & \text{– for long – term actions} \end{cases}$

$\sum b_{eff}$ is the total effective steel plate area, accounting for shear lag.

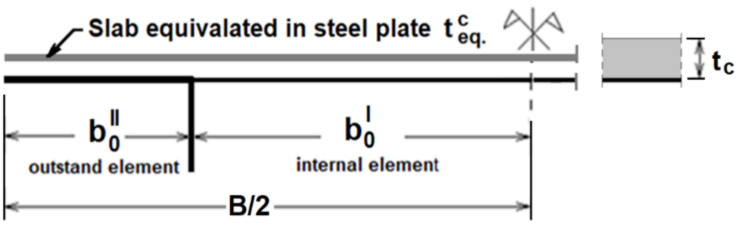

Figure 3. Equivalent steel representation of composite orthotropic deck

4.4. Creep and Concrete Shrinkage Stresses

Figure 4 shows the calculation scheme for stresses due to concrete creep and shrinkage. [9]

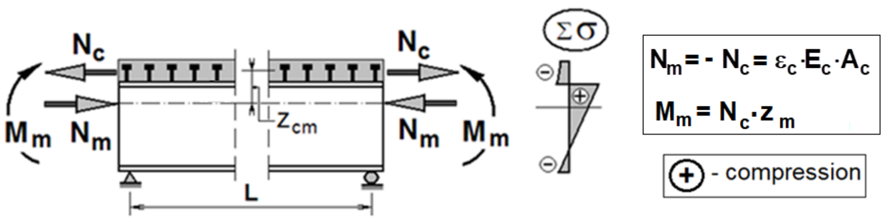

Figure 4. Development of stresses due to concrete creep and shrinkage

Stresses at the slab center and extreme fibers of the steel box girder are:

$$\sigma_c = -\frac{N_c}{A_c} + \frac{1}{n}\left(\frac{N_m}{A_m} + \frac{M_m}{I_m} z_{cm}\right) \tag{9}$$

$$\sigma_{a.sup} = \frac{N_m}{A_m} + \frac{M_m}{I_m} z_{as}; \; \sigma_{a.inf} = \frac{N_m}{A_m} - \frac{M_m}{I_m} z_{ai} \quad (10.a; b)$$

4.5. Stresses Induced by Vertical Temperature Components

The strain from temperature variation is:

$$t_{eq.}^{c} = \frac{A_{c.eff}}{n \cdot (B/2)} = \frac{t_c \cdot \sum b_{eff}}{n \cdot (0.5B)} \quad (11)$$

where: $\alpha_T = 1 \cdot 10^{-5} / ^0 C$ is the thermal expansion coefficient of concrete and steel in composite structures ([8], Annex C, Table C.1).

For composite decks, the following values apply [10]:

- $\Delta T_{M.Heating} = 15°C$
- $\Delta T_{M.Cooling} = 18°C$

Figure 5 [11] shows stresses on the composite section when the concrete is colder than the opposite side. If the deck is warmer, stresses reverse.

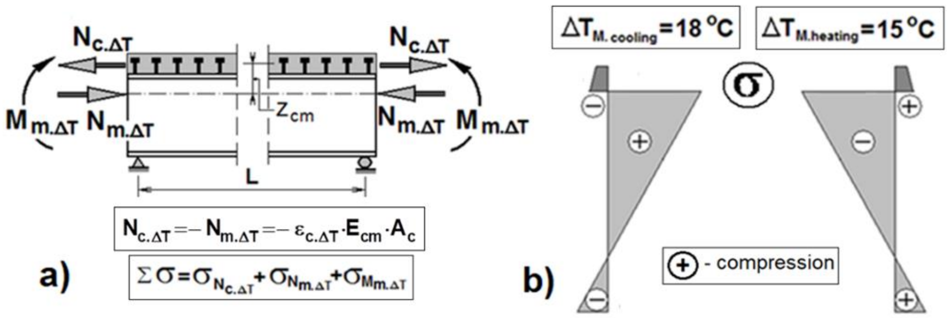

Figure 5. Development of stresses due to thermal effects on composite girder depth

5. CASE STUDY: COMPOSITE STEEL-CONCRETE ORTHOTROPIC DECK

Examples of shear lag phenomena in orthotropic steel plates are presented in [12]. An orthotropic steel structure for a footbridge deck was analyzed in [9].

In this case study, a similar structure with a composite steel-concrete deck is analyzed.

The footbridge superstructure is a simply supported composite steel-concrete girder with a span of 38.00 m. The steel grade used is S355 (Figure 6).

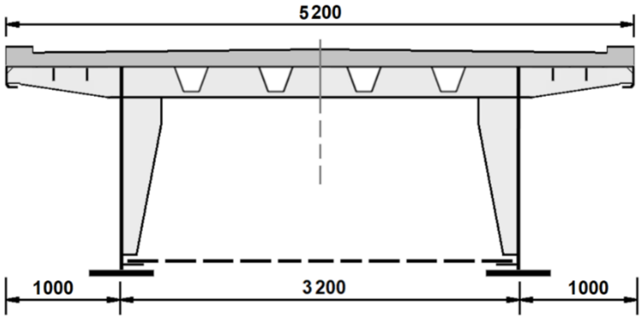

Figure 6. Cross-section of superstructure

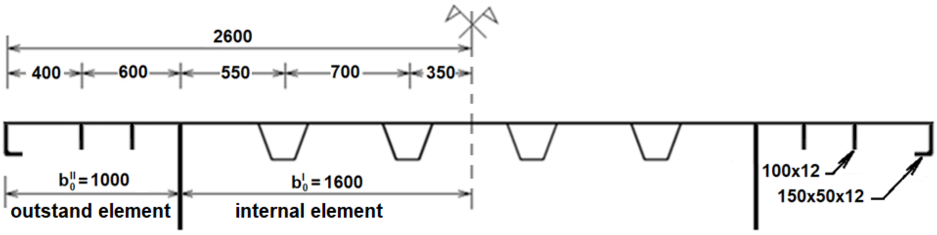

Figure 7. Steel deck dimensions

The steel deck dimensions and the component elements are presented in Figure 7.

Since $b_0 > L_e/50$ (where $L_e/50 = 400$ mm), shear lag must be considered.

5.1. Elastic Shear Lag at Serviceability Limit State and Fatigue (SLS)

The dimensions of steel deck panels are presented and gross area of subpanels is calculated (Figures 8-9).

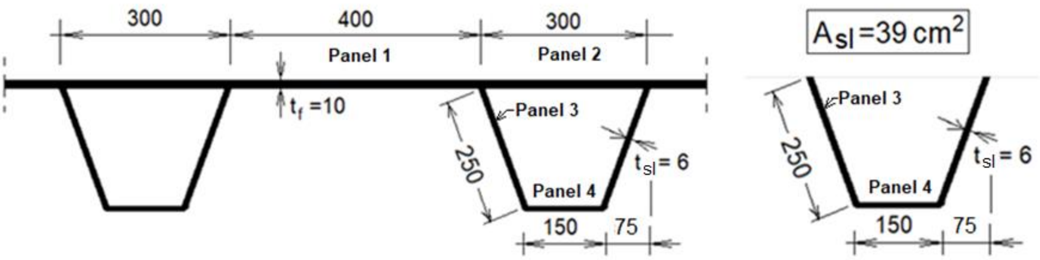

Figure 8. Dimensions of Steel Deck Panels

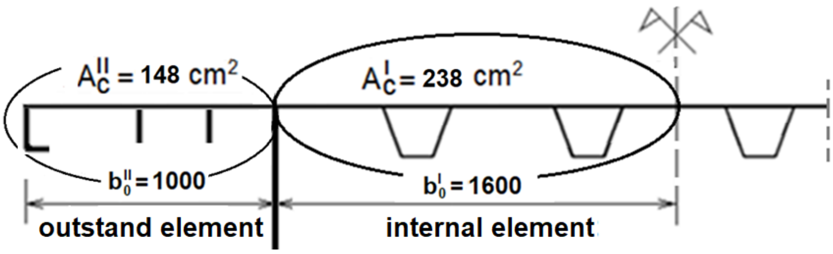

Figure 9. Gross Cross-Section Area of Steel Deck

5.2. Effective[s] width and the shear lag at serviceability limit state (SLS)

The coefficients α_0 for internal (I) and outstand (II) elements of the orthotropic plate are:

$$\alpha_0^I = \sqrt{1+\frac{2\cdot 39}{160\cdot 1.0}} = 1.22\,; \qquad \alpha_0^{II} = \sqrt{1+\frac{1\cdot 39+2\cdot 12+1\cdot 24}{100\cdot 1.0}} = 1.37$$

For an effective length L_e=38.00 m, it is obtained as follows:

- Internal element:

$$k_I = \frac{\alpha_0^I\cdot b_0^I}{L_e} = \frac{1.22\cdot 160}{3800} = 0.05\,;\; \beta^I = \beta_1^I = \frac{1}{1+6.4\cdot k^2} = \frac{1}{1+6.4\cdot 0.05^2} = 0.98$$

$$b_{eff}^I = \beta_1^I\cdot b_0^I = 0.98\cdot 1600 = 1568\,\text{mm}$$

- Outstand element:

$$k_I = \frac{\alpha_0^{II}\cdot b_0^{II}}{L_e} = \frac{1.37\cdot 100}{3800} = 0.036\,;\; \beta = \beta_1 = \frac{1}{1+6.4\cdot k^2} = \frac{1}{1+6.4\cdot 0.036^2} = 0.99$$

$$b_{eff}^{II} = \beta_1^{II}\cdot b_0^{II} = 0.99\cdot 1100 = 1089\,\text{mm}$$

Using simplified formulas, results are very close, confirming the entire deck plate is active.

$$b_{eff} = \min\left(b_0; \frac{L}{8}\right) = b_0^{I,II} = \begin{cases} 1600\,\text{mm} - \text{for internal element} \\ 1000\,\text{mm} - \text{for outstand elment} \end{cases}$$

5.3. Shear Lag Effect for Ultimate Limit States (ULS - Model 2)

Model 2 (Method c from [5]) for the ultimate limit states verification of the orthotropic plate is used: interaction between shear lag and plate buckling.

Calculation of the effective[p] area of subpanels

- Panel 1:

$$\bar{\lambda}_{p1} = \frac{b_1/t}{28.4\cdot\varepsilon\cdot\sqrt{k_\sigma}} = \frac{400/10}{28.4\cdot 0.81\cdot\sqrt{4}} = 0.869 > 0.673$$

$$\rho_1 = \frac{\bar{\lambda}_{p1} - 0.055\,(3+\Psi)}{\bar{\lambda}_{p1}^2} = \frac{0.869 - 0.055\,(3+1)}{0.869^2} = 0.86$$

$$\Rightarrow b_{1.eff} = \rho_1\cdot b_1 = 0.86\cdot 400 = 344\text{mm}.$$

- Panel 2:

$$\bar{\lambda}_{p2} = \frac{b_2/t}{28.4\cdot\varepsilon\cdot\sqrt{k_\sigma}} = \frac{300/10}{28.4\cdot 0.81\cdot\sqrt{4}} = 0.326 < 0.673 \Rightarrow \rho_2 = 1$$

- Panel 3:

$$\bar{\lambda}_{p3} = \frac{b_3 / t_{s\ell}}{28.4 \cdot \varepsilon \cdot \sqrt{k_\sigma}} = \frac{250/6}{28.4 \cdot 0.81 \cdot \sqrt{4}} = 0.906 > 0.673$$

$$\rho_3 = \frac{\bar{\lambda}_{p.3} - 0.055 \ (3+\Psi)}{\bar{\lambda}^2_{p3}} = \frac{0.906 - 0.055 \ (3+1)}{0.906^2} = 0.836$$

$$\Rightarrow b_{3.eff} = \rho_3 \cdot b_3 = 0.836 \cdot 250 = 210\text{mm}.$$

- Panel 4:

$$\bar{\lambda}_{p4} = \frac{b_4 / t_{s\ell}}{28.4 \cdot \varepsilon \cdot \sqrt{k_\sigma}} = \frac{150/6}{28.4 \cdot 0.81 \cdot \sqrt{4}} = 0.543 < 0.673 \Rightarrow \rho_4 = 1$$

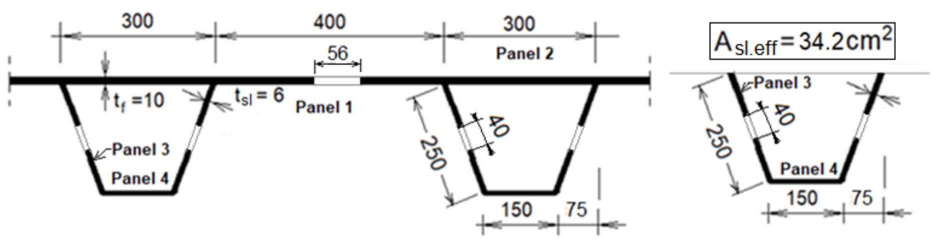

Figure 10. Effective^p panel areas

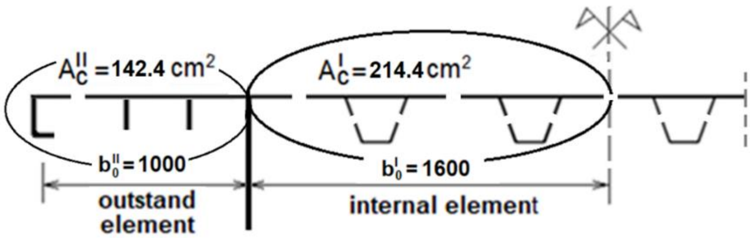

Figure 11. Effective^p panel areas of internal and outstand elements

5.4. Effectives width and the shear lag at ultimate limit state (ULS)

The effect of plate buckling in the elastic global analysis and ULS may be neglected because the condition: $A_{eff} > \rho_{lim} \cdot A_f = 0.5 \cdot A_f$ [13], is fulfilled.

For a more exact evaluation of shear lag effect the Method c) recommended by EN1993-1-5 is used.

An elastoplastic reduction factor $\beta^k \geq \beta$ is directly applied to the effective^p area of the compression flange, where k is based on α_0:

$$A_{eff} = \beta^k \cdot A_{c.eff} \geq A_{c.eff} \cdot \beta \quad \text{or:} \quad A_{eff} = \beta_{e-p} \cdot A_{c.eff}; \ \beta_{e-p} = \max(\beta^k; \beta).$$

From the Figure 11 it is obtained:

$$A_{eff}^{I,II} = \begin{cases} 0.98^{0.05} \cdot 214.4 = 214\,cm^2 > 0.98 \cdot 214.4 = 202\,cm^2 & -\text{for internal element} \\ 0.99^{0.036} \cdot 142.4 = 142.3 > 0.99 \cdot 142.4 = 141\,cm^2 & -\text{for outstand element} \end{cases}$$

It can be noticed that in this case the difference between A_{eff} and $A_{c.eff}$ is negligible.

Given the results and the fact that the entire plate width is active, in the ULS method, the orthotropic plate will be replaced with equivalent flat plates [13], [14].

Practically, the analyzed orthotropic deck is replaced with two plates of equivalent thickness (Figure 12):

- Central plate:

$$t_{eq.I}^{ULS} = \frac{A_{eff}^{I}}{b_0^{I}} = \frac{214}{160} = 1.34\,cm \approx 14\,mm$$

- Cantilever plate:

$$t_{eq.II}^{ULS} = \frac{A_{eff}^{II}}{b_0^{II}} = \frac{142.3}{100} = 1.42\,cm \approx 14\,mm$$

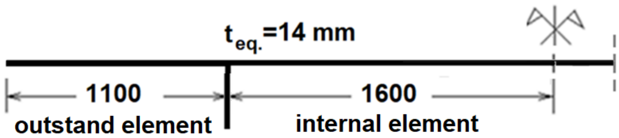

Figure 12. Steel section of orthotropic deck for ULS calculation

5.5. Composite deck

Elastic and plastic analysis of composite steel-concrete girders is presented in [15, 16].

The reinforced concrete slab (Figure 13) is replaced by an equivalent steel plate. For a 160 mm thick C30/37 concrete slab:

$$n = \begin{cases} n_0 = \dfrac{E_a}{E_{cm}} = \dfrac{210}{33} = 6.36 & -\text{for short}-\text{term actions} \\ n_L = n_0 \cdot (1 + \psi_L \cdot \phi(t, t_0)) = 6.36 \cdot 3.76 \approx 24 & -\text{for long}-\text{term actions} \end{cases}$$

$$t_{eq.}^{c} = \begin{cases} 28\,mm & -\text{for short}-\text{term actions} \\ 7.5\,mm & -\text{for long}-\text{term actions} \end{cases}$$

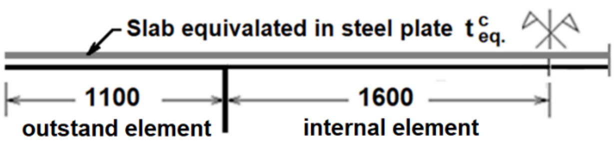

Figure 13. Equivalent Steel Representation of Composite Orthotropic Deck

Stresses are evaluated based on assembly and installation technology. Plastic field calculations apply to Class 1 and 2 cross-sections; elastic field calculations apply to Class 3 and 4.

6. ORIGINAL CONTRIBUTIONS

This paper presents several original contributions to the analysis and design of composite steel-concrete orthotropic decks, with specific applicability in pedestrian bridges. The main original elements include:

a) Application of Eurocode-based Methodology to Orthotropic Composite Decks

A unified analytical methodology is proposed, adapted from the EN 1993-1-5 and EN 1994 standards, for composite steel-concrete orthotropic decks, which are not explicitly treated in these norms. The paper extends the application of Eurocode provisions to a specific case of footbridge deck design with orthotropic plates, by interpreting and correlating different limit state verifications (SLS and ULS).

b) Advanced Evaluation of Shear Lag Effects

The study provides a detailed assessment of shear lag effects, both in serviceability (SLS) and ultimate (ULS) limit states, using simplified and advanced models recommended in EN 1993-1-5.

c) Integration of Thermal and Rheological Stresses in Composite Analysis

The paper accounts for creep, shrinkage, and thermal gradient effects on the composite section, presenting their cumulative influence in design.

d) Case Study on a 38 m Composite Footbridge

A full-scale parametric case study was carried out for a simply supported pedestrian bridge with a 38-meter span. The structural configuration, detailing, effective widths, and orthotropic plate behavior were analyzed comprehensively, demonstrating that the entire plate width is active in load transfer. This result confirms the applicability of simplified assumptions in practical bridge design.

e) Design Simplification through Equivalent Plate Transformation

A practical design simplification is introduced by replacing the orthotropic plate with two flat plates of equivalent stiffness, allowing direct application of classical composite beam theory.

7. CONCLUSIONS

The analysis of composite steel-concrete orthotropic decks demonstrates their significant advantages in modern bridge engineering, particularly for pedestrian bridges and medium-span structures. The key findings and recommendations are summarized below:

Key Advantages

a) Enhanced Structural Performance

- The composite action between the orthotropic steel deck and concrete slab substantially improves bending and torsional stiffness, leading to more efficient load distribution;
- The steel plating serves dual roles as structural reinforcement and formwork, reducing construction time and costs.

b) Simplified Construction

- Eliminates the need for temporary bracing during assembly, streamlining the erection process;
- Lightweight prefabricated sections allow for single-unite installation, minimizing disruptions in environmentally sensitive areas (e.g., riverbeds).

c) Durability and Maintenance

- The concrete slab protects the steel upper flanges from corrosion, extending the structure's service life;
- Reduced susceptibility to dynamic vibrations improves pedestrian comfort in footbridge applications.

While the study is theoretical, the results were corroborated by existing experimental findings in the literature. The analytical model was applied to a realistic case study of a pedestrian footbridge with a 38 m span, demonstrating full activation of the orthotropic deck and validating the model assumptions. Future work will include experimental validation on scaled models or in-situ monitoring of similar structures to confirm the theoretical conclusions.

REFERENCES

[1]. EN 1994-1-1: 2006. Eurocode 4: *Design of composite steel-concrete structures – Part 1-1: General rules and rules for buildings*

[2]. EN 1994-2: 2006. Eurocode 4: *Design of composite steel-concrete structures – Part 2: General rules and rules for bridges*

[3]. ŞT. GUŢIU, P. MOGA, A.D. DANCIU, C. MOGA: *Lateral Torsional Buckling Resistance of Steel Plate Girders according to Euronorms*. The 8th International

Conference "Bridges in Danube Basin". Springer Vieweg. ISBN 978-3-658-03713-0. Timisoara. 2013.

[4]. C. MOGA, ŞT. GUŢIU, A.D. DANCIU: *Influence of cross-sectional shape on the values of the critical buckling force*. 14th International Multidisciplinary Scientific Geoconference (SGEM 2014), Nano, Bio and Green – Technologies for a Sustainable Future, 17 June - 26 July, 2014, Bulgaria, Conference Proceedings, WOS:000366135800029, ISSN 1314-2704.

[5]. EN 1993-1-5: 2008. Eurocode 3: Design of steel structures – Part 1-5: *Plated structural elements*

[6]. P. MOGA, ŞT. I. GUŢIU, F. ANGHEL, C. MOGA, A.D. DANCIU: *Footbridge over the Somes River in Cluj-Napoca, Romania*, The 9th International Conference "Bridges in Danube Basin", 2016, published in "Procedia Engineering 156 (2016)" ELSEVIER, ISSN 1877-7058, DOI: 10.1016/j.proeng.2016.08.259, p. 249-256

[7]. ŞT. I. GUŢIU, C. MOGA, A.D. DANCIU, M. SUCIU: *Constructive solutions for medium span footbridges*. 16th International Multidisciplinary Scientific Geoconference (SGEM 2016), Nano, Bio and Green – Technologies for a Sustainable Future, 30 June-6 July, 2016, Bulgaria, Conference Proceedings, Volume II, Green buildings technologies and materials; Green design and sustainable architecture, ISBN 978-619-7105-69-8, ISSN 1314-2704, pp 517-524

[8]. C. MOGA, Crina FENEȘAN, M. SUCIU: *Shear lag and local buckling interaction in orthotropic deck of steel bridges*. Buletinul Univ. Tehn. „Gh. Asachi". Vol. 67. Nr. 1/2021. SCIENDO. DOI: 10.2478/bipca-3021-0006

[9]. I. VAYAS, A. ILIOPOLOS: *Design of Steel-Concrete Composite Bridges to Eurocodes*. CRC Press. Taylor & Francis Group. 2013

[10]. EN 1991-1-5: Actions on structures. Part 1-5: *General actions -Thermal actions*

[11]. C. MOGA, ŞT. I. GUŢIU, Alexandra DANCIU, M. SUCIU: *Concrete shrinkage stresses and thermal effects in the composite girders according to Eurocodes*, 16th International Multidisciplinary Scientific Geoconference (SGEM 2016), Nano, Bio and Green – Technologies for a Sustainable Future, 30 june-6 july, 2016, Bulgaria, Conference Proceedings, Volume II, Green buildings technologies and materials; Green design and sustainable architecture, ISBN 978-619-7105-69-8, ISSN 1314-2704, pp 501-508

[12]. C. MOGA, Claudia ALB, M. SUCIU: *Effect of design parameters on shear lag in orthotropic deck of steel road bridges*. Buletinul Univ. Tehn. „Gh. Asachi". Vol. 67. Nr. 2/2021. SCIENDO. DOI: 10.2478/bipca-3021-0018, pag. 95-104

[13]. D. BEG, U. KUHLMANN, L. DAVAINE, B. BRAUN: *Design of Plated Structures*. ECCS. 2010

[14]. B. JOHANSSON, R. MAQUOI, G. SEDLACEK, C. MÜLLER, D. BEG: *Commentary and worked examples to EN 1993-1-5 „Plated structural elements*" (Programme of CEN/TC 250). 2007

[15]. ŞT. I. GUŢIU, C. MOGA, Alexandra D. DANCIU: *Elastic and plastic design of composite steel-concrete girders with circular holes*, 16th International Multidisciplinary Scientific Geoconference (SGEM 2016), Nano, Bio and Green – Technologies for a Sustainable Future, 30 june-6 july, 2016, Bulgaria, Conference Proceedings, Volume II, Green buildings technologies and materials; Green design and sustainable architecture, ISBN 978-619-7105-69-8, ISSN 1314-2704, pp 549-556

[16]. P. MOGA, ŞT. GUŢIU, C. MOGA: *Footbridges*, 2020. Cluj-Napoca, Ed. UT Press